# Frequency Based Design of KDamper for Seismic Isolation of a Single Pier Concrete Bridge

**Evangelos Sapountzakis**, *Professor, National Technical University of Athens/Institute of Structural Analysis and Antiseismic Research/School of Civil Engineering, Zografou Campus, Athens, Greece; email: cvsapoun@central.ntua.gr*

**Panagiota Syrimi**, *PhD Candidate, National Technical University of Athens/Institute of Structural Analysis and Antiseismic Research/School of Civil Engineering, Zografou Campus, Athens, Greece; email: panagiota.syrimi@gmail.com*

**Ioannis Antoniadis**, *Professor, National Technical University of Athens/Mechanical Design and Control Systems Section/Mechanical Engineering Department, Zografou Campus, Athens, Greece; email: antogian@central.ntua.gr*

**ABSTRACT**: *Contemporary seismic isolation systems for bridge applications provide a) horizontal isolation from earthquake shaking effects, and b) energy dissipation mechanisms to reduce displacements. Throughout the years, many kinds of seismic isolation mechanisms have been developed, with those incorporating negative stiffness elements being the most promising ones. The negative stiffness behaviour is achieved through special mechanical designs involving conventional positive stiffness pre-stressed elastic mechanical elements, arranged in appropriate geometrical configurations. In this context, a novel passive vibration isolation and damping concept is introduced, the KDamper, whose main advantage is that no reduction in the overall stiffness of the system is required. In this paper, the application of the KDamper concept on a typical concrete bridge with conventional bearings, to mitigate seismic effects, is considered. The system's design is based on frequency domain analysis of both the initial and the isolated bridge structure. Comparative results between the two systems confirm that the proposed device can provide a promising alternative to conventional techniques, offering numerous advantages, such as increased damping and simple technological implementations.*

**KEYWORDS:** Seismic Isolation, Negative Stiffness, Bridge, Frequency Domain, KDamper

**SITE LOCATION:** Geo-Database

## INTRODUCTION

In response to the damage generated by earthquakes occurring in densely populated areas, seismic design codes for buildings, bridges and infrastructure changed towards the design of structures with better seismic performance. Seismic isolation appears to be the most promising alternative to conventional antiseismic techniques, as it is based on the concept of reducing the seismic demand rather than increasing the earthquake resistance capacity of the structure. Focusing on bridge structures, contemporary seismic isolation systems follow the basic principles of earthquake mitigation, thus, providing a) horizontal isolation, by decoupling the bridge deck from substructure, and b) an energy dissipation mechanism to reduce displacements. Throughout the last decades, a variety of isolation devices including elastomeric bearings (with and without lead core), frictional/sliding bearings, roller bearings and most recently tunes mass damper (TMD) devices, has been developed. Furthermore, the significant advance of mechanical expertise has facilitated the implementation of more complex devices, such as newly-fabricated hardware incorporating negative stiffness elements.

Tuned Mass Dampers (TMDs) were first applied by Frahm (1909), whereas an optimal design theory for such configurations has been proposed by Den Hartog (1956). Since then, TMDs have been frequently used to absorb vibrations of skyscrapers

Submitted: 30 July 2017; Published: 26 November 2018
Reference: Sapountzakis, E., Syrimi, P. and Antoniadis, I. (2018). *Frequency Based Design of KDamper for Seismic Isolation of A Single Pier Concrete Bridge*. International Journal of Geoengineering Case Histories, Vol.4, Issue 4, p.289-305. doi: 10.4417/IJGCH-04-04-05

under earthquake and wind loading [Qin et al. (2009), McNamara (1979), Luft (1977)], with Taipei 101 Tower (101 stories, 504 m) in Taiwan (Haskett et al. 2003), one of the tallest buildings worldwide, being the most characteristic example of TMD implementation. More recently, the use of TMDs has been included in studies concerning mitigation of the effects of seismic or other kinds of excitation on bridge structures (Debnath et al. 2015). The basic design principle of TMD mechanisms lies on the tuning of the device's natural frequency in resonance with the fundamental frequency of the primary structure, aiming to the transfer of a large amount of the structural vibrating energy to the TMD device. This energy is then dissipated through damping. Besides the effectiveness of such devices, TMDs suffer from two main disadvantages: a) detuning phenomena: even slight changes of environmental or other external parameters may disturb the tuning and lead to deterioration of the device's performance (Weber et al. 2010), and b) difficulty during construction and placement due to the large oscillating mass, required to achieve the desired vibration reduction.

The last steps towards vibration absorption include the introduction of negative stiffness elements to seismic isolation mechanisms. True negative stiffness is defined as a force that assists motion instead of opposing it, as in the case of a positive stiffness spring. Starting from the work of Molyneaux (1957) and Platus (1999), the basic idea behind the incorporation of negative stiffness elements is the significant reduction of the stiffness that consequently leads to the reduction of the natural frequency of the system even at almost zero levels, resulting in configurations as in Carella et al. (2007), namely, "Quazi Zero Stiffness" (QZS) oscillators. Enhanced vibration isolation is, thus, achieved due to the fact that the transmissibility of the system for all operating frequencies above the natural one is reduced. An initial comprehensive review of such designs can be found in Ibrahim (2008). The negative stiffness behaviour is primarily achieved by special mechanical designs involving conventional positive stiffness pre-stressed elastic mechanical elements, such as post-buckled beams, plates, shells and pre-compressed springs, arranged in appropriate geometrical configurations. However, the basic drawback that QZS oscillators present is their fundamental requirement for a drastic reduction of the stiffness of the structure almost to negligible levels, limiting its static load capacity.

In an effort to combine the advantages of the two previously described mechanisms, a novel passive vibration isolation and damping concept, entitled KDamper concept, has been proposed in Antoniadis et al. (2015) and Antoniadis et al. (2016). The proposed device is characterized by the incorporation of a negative stiffness element and exhibits extraordinary damping properties, without presenting the drawbacks of either TMDs or QZS oscillators. The novelty of the KDamper concept lies on the appropriate redistribution of the individual stiffness elements and the reallocation of damping. The inherent instability that usually accompanies configurations with negative stiffness elements is hereby avoided, as the proposed device is designed to be both statically and dynamically stable. Moreover, as the KDamper's tuning is controlled by the negative stiffness element's parameters, any detuning phenomena - the major disadvantage of the TMDs – are avoided. Once such a configuration is designed according to the approach proposed in Antoniadis et al. (2016), the isolated system exhibits a significantly improved dynamic and damping behavior. A first approach to the implementation of the KDamper concept for the seismic isolation of a typical bridge with and without flexible piers can be found in Sapountzakis et al. (2017) and Sapountzakis et al. (2016), respectively.

In this paper, the implementation of the KDamper concept to the mitigation of the effects of seismic excitation on bridge structures is considered, by applying the KDamping concept to a typical concrete bridge with conventional bearings. The design is based on the improvement of the frequential characteristics of the structure. The negative stiffness element is realized by a non-linear bistable element, which operates around an unstable equilibrium point. More specifically, this bistable element takes the form of two symmetric linear horizontal springs, connected with the rest of the elements through an appropriate articulated mechanism. The dynamic response of the bridge is examined before and after the implementation of seven KDamper devices that replace the conventional bearings. Finally, the resulting system's damping ratio is calculated and the transfer functions of both the initial and the isolated systems are presented.

## METHODOLOGY

### Overview Of The KDamper Concept

Figure 1 presents the basic layout of the proposed vibration isolation and damping concept. The device is designed to minimize the response $x(t)$ of mass $m_s$ and static stiffness $k_o$ to a base excitation of $x_G(t)$. The single degree of freedom (SDoF) system may be undamped or have a low initial damping ratio.

The basic requirement of the KDamper is that the overall static stiffness of the system is maintained. This is algebraically expressed as follows

$$k_R + \frac{k_e k_N}{k_e + k_N} = k_o \tag{1}$$

where $k_R$ and $k_e$ represent the stiffness coefficients of the conventional springs, $k_N$ is the algebraic value of the stiffness coefficient of the negative stiffness element and $k_o$ stands for the stiffness of an equivalent undamped initial SDoF system. The aforementioned requirement is introduced for comparison reasons between the two cases (initial and isolated one).

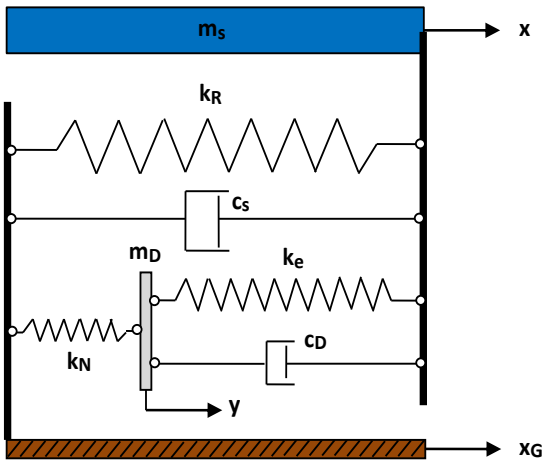


*Figure 1. Schematic representation of the considered vibration absorption concept.*

The equations of motion after the implementation of the KDamper are presented below.

$$m_s\ddot{u}_s + (c_s + c_D)\dot{u}_s - c_D\dot{u}_D + (k_R + k_e)u_s - k_e u_D = -m_s\ddot{x}_G \tag{2}$$

$$m_D\ddot{u}_D - c_D\dot{u}_s + c_D\dot{u}_D - k_e u_s + (k_e + k_N)u_D = -m_D\ddot{x}_G \tag{3}$$

where

$$u_s = x - x_G \tag{4}$$

$$u_D = y - x_G \tag{5}$$

In the previous equations, $c_s$ is the initial's systems damping coefficient and $c_D$ is the damping coefficient of the additional damper.

At this point, it should be mentioned that the KDamper essentially consists of an indirect approach to increase the inertia effect of the additional mass $m_D$ without, however, increasing directly the mass $m_D$ itself, as negative stiffness elements contribute to the desired increase of inertia forces, too.

**Proposed Design Approach For The KDamper And Basic Properties**

The device's behavior and consequently, the isolated system's dynamic performance, are controlled by three basic design parameters, $\mu$, $\kappa$ and $\rho$. Parameters $\mu$ and $\kappa$ are defined as follows:

$$\mu = \frac{m_D}{m_s} \tag{6}$$

$$\kappa = -\frac{k_N}{k_e + k_N} \tag{7}$$

where $m_s$ is the superstructure's mass and $m_D$ is the additional mass of the KDamper, as shown in Figure 1. The mass ratio $\mu$, is selected arbitrarily by the user. The larger the value of $\mu$ and consequently the value of $m_D$, the better the results of the system's dynamic response. However, when applying to structures where the value of $m_s$ is extremely large, such as bridges, a careful choice satisfying both the desired effects on structure's response and the ability to construct and place the device should be made.

Considering parameter $\kappa$, further explanation on how to choose the right value is provided later in this paper. Frequency ratio $\rho$ is defined as

$$\rho = \frac{\omega_D}{\omega_o} \tag{8}$$

where

$$\omega_o = \sqrt{\frac{k_o}{m_s}} \tag{9}$$

$$\omega_D = \sqrt{\frac{k_D}{m_D}} \tag{10}$$

and

$$k_D = k_e + k_N \tag{11}$$

For each set of the parameters $\mu$ and $\kappa$, the value of $\rho$ is derived from

$$\rho(\kappa, \mu) = \sqrt{-\frac{C_\rho}{B_\rho}} \tag{12}$$

where coefficients $C_\rho$ and $B_\rho$ are calculated according to the procedure described in Sapountzakis et al. (2017). Further information on the properties and derivation of the parameter $\rho$ can be found in Antoniadis et al. (2016).

Considering the selection of $\zeta_D$, defined in Equation (13), numerous approaches are possible, the detailed treatment of which is beyond the scope of the current paper. In this effort, $\zeta_D$ is calculated numerically.

$$\zeta_D = \frac{c_D}{2\sqrt{k_D m_D}} \tag{13}$$

Finally, following the steps described in the Appendix A of Sapountzakis et al. (2017), the values of the KDamper's elements are given by

$$\frac{k_N}{k_o} = \kappa_N = -\kappa\mu\rho^2 \tag{14}$$

$$\frac{k_e}{k_o} = \kappa_e = (1+\kappa)\mu\rho^2 \tag{15}$$

$$\frac{k_R}{k_o} = \kappa_R = 1 + \kappa(1+\kappa)\mu\rho^2 \tag{16}$$

$$m_D = \mu m_s \tag{17}$$

$$c_D = 2\zeta_D\sqrt{(k_e + k_N)m_D} \tag{18}$$

where $\mu$, $\kappa$ and $\rho$ are the parameters defined in Equations (6), (7) and (8), respectively. Equation (18) is derived after substituting Equation (11) into Equation (13).

At this point, some useful KDamper properties, also mentioned in Sapountzakis et al. (2017), are reminded, aiming to assist the reader and ensure understanding of the proposed frequency based design procedure. Concerning the parameter $\kappa$, it should be mentioned here that increasing its value has a number of implications in the design of the KDamper. First, it results in high stiffness values, as presented in Figures 2-4. In addition, as observed in Figure 5, when $\kappa$ reaches $\kappa_{max}$ the frequency ratio $\rho$ tends to infinity. The value of $\kappa$ is, also, responsible for the shift of the eigenfrequency (and by extension the shift of the eigenperiod) of the isolated system. This can be observed in Figures 6 and 7, where the effect of the value of $\kappa$ to the transfer function of the isolated system is depicted, in terms of acceleration and displacement, respectively.

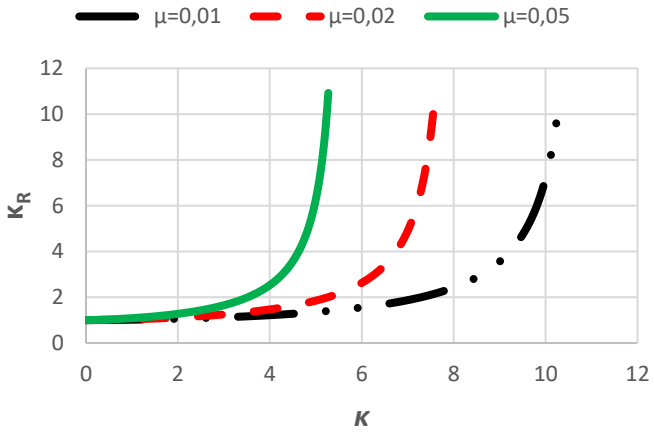


*Figure 2. Increase of the value of stiffness coefficient $k_R$ by increasing $\kappa$ (in terms of ratio $\kappa_R$).*

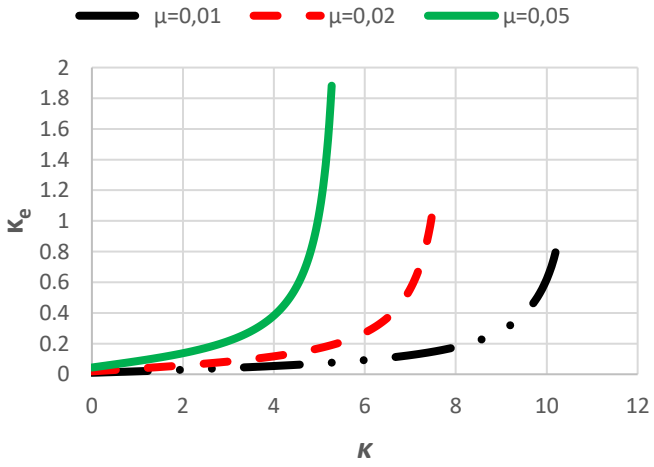


*Figure 3. Increase of the value of stiffness coefficient $k_e$ by increasing $\kappa$ (in terms of ratio $\kappa_e$).*

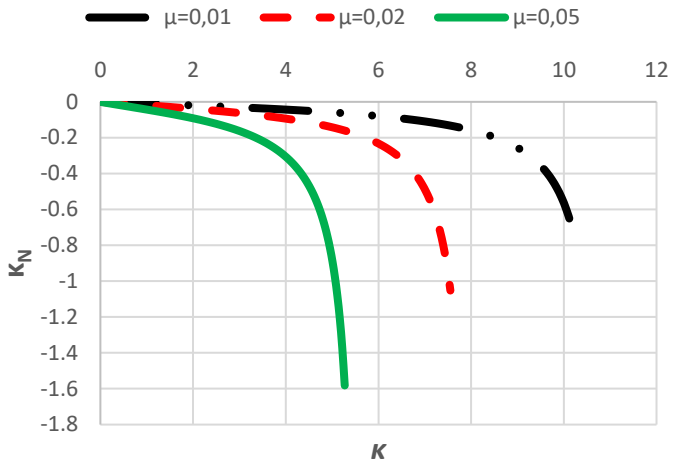


*Figure 4. Increase of the value of negative stiffness coefficient $k_N$ by increasing κ (in terms of ratio $\kappa_N$).*

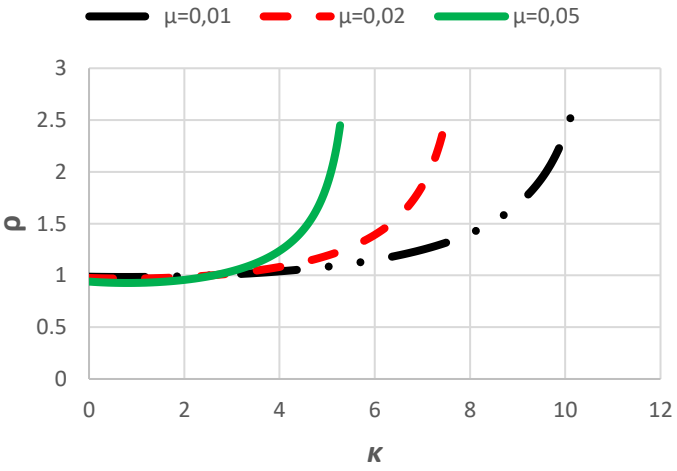


*Figure 5. Variation of the KDamper's parameters μ and κ over the frequency ratio $\rho = \frac{\omega_D}{\omega_o}$.*

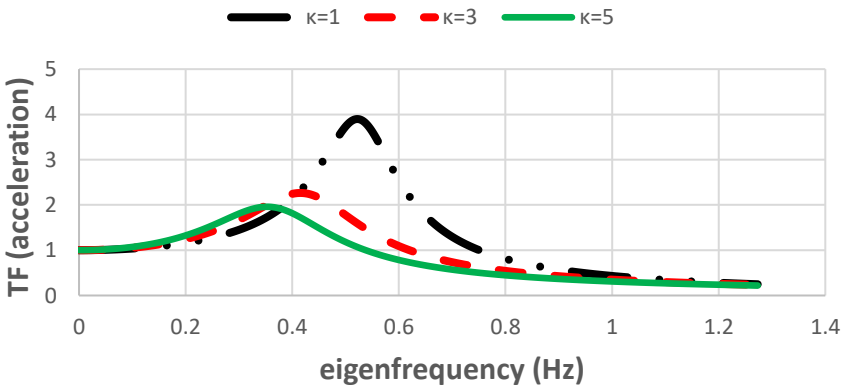


*Figure 6. Transfer function of the isolated system in terms of acceleration.*

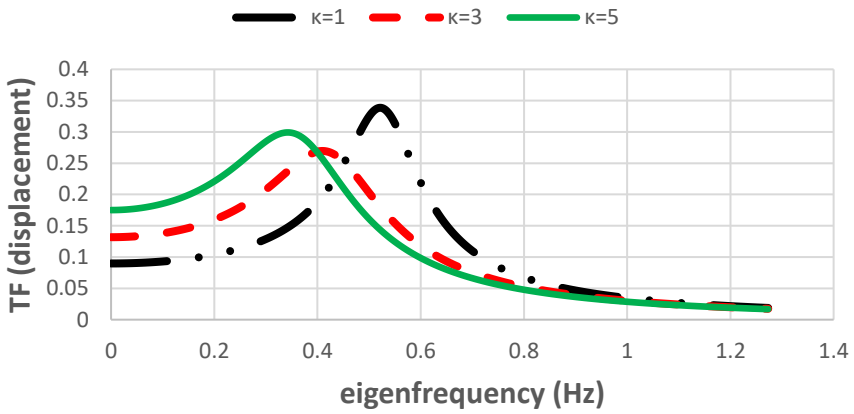


*Figure 7. Transfer function of the isolated system in terms of displacement.*

Increasing the stiffness and especially $k_N$, may endanger the static stability of the structure. Although $k_N$ is selected according to Equation (1) to ensure the system's static stability, variations of $k_N$ result in practice due to various reasons, such as temperature variations, manufacturing tolerances, or non-linear behavior, since almost all negative stiffness designs result from unstable non-linear systems. Consequently, an increase of the absolute value of $k_N$ by a factor $\varepsilon$ may lead to a new value of $k_{NL}$ where the structure becomes unstable, given by

$$k_R + \frac{k_e k_{NL}}{k_e + k_{NL}} = 0 \Leftrightarrow k_{NL} = -\frac{k_R k_e}{k_R + k_e} = (1+\varepsilon)k_N \tag{19}$$

Substitution of Equations (14) – (16) into Equation (19) leads to the following estimate for the static stability margin $\varepsilon$

$$\varepsilon = \frac{1}{\kappa[1+(1+\kappa)^2 \mu \rho^2]} \tag{20}$$

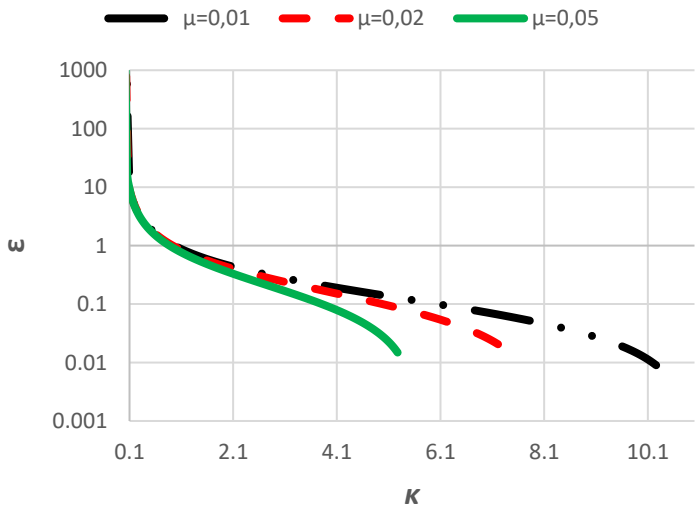


*Figure 8. Variation of the KDamper's parameters μ and κ over the static stability margin ε.*

Figure 8 presents the variation of $\varepsilon$ over $\kappa$ and $\mu$. As observed from Equation (11) and Figure 8, the increase of the negative stiffness of the system is upper bounded by the static stability limit of the structure, where $\varepsilon$ tends to zero. The increase of the value of $\kappa$ is, consequently, upper limited by a value of $\kappa_{max}$. In practice, $\kappa_{max}$ can be calculated by a Goal Seek command with the condition that $\varepsilon$ is equal to zero. In this effort, the value of $\kappa$ is selected so that the resulting eigenfrequency of the isolated structure is equal to 0.4 Hz. The reason why this particular value of eigenfrequency is chosen is that, according to Figures 6 and 7, the value of 0.4 Hz results in improved dynamic performance of the isolated structure in both terms of acceleration and displacement. From the same figures, it can also be noticed that, even though, systems with eigenfrequency lower than 0.4 Hz exhibit an enhanced behavior in terms of accelerations, they demonstrate an undesired increase of displacements.

## IMPLEMENTATION FOR SEISMIC ISOLATION

### Test Case Considered

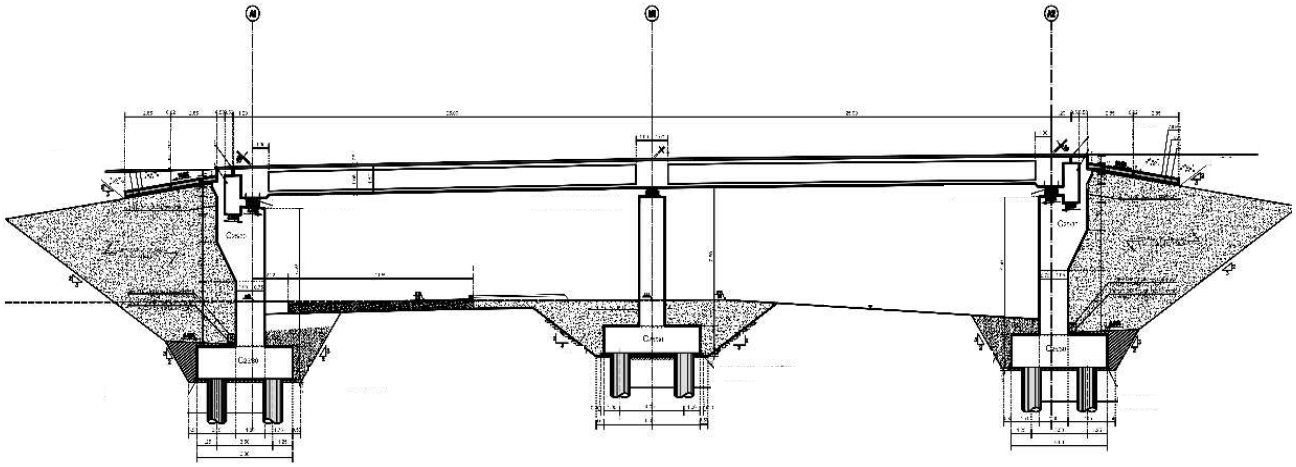

*Figure 9. Bridge considered: longitudinal section.*

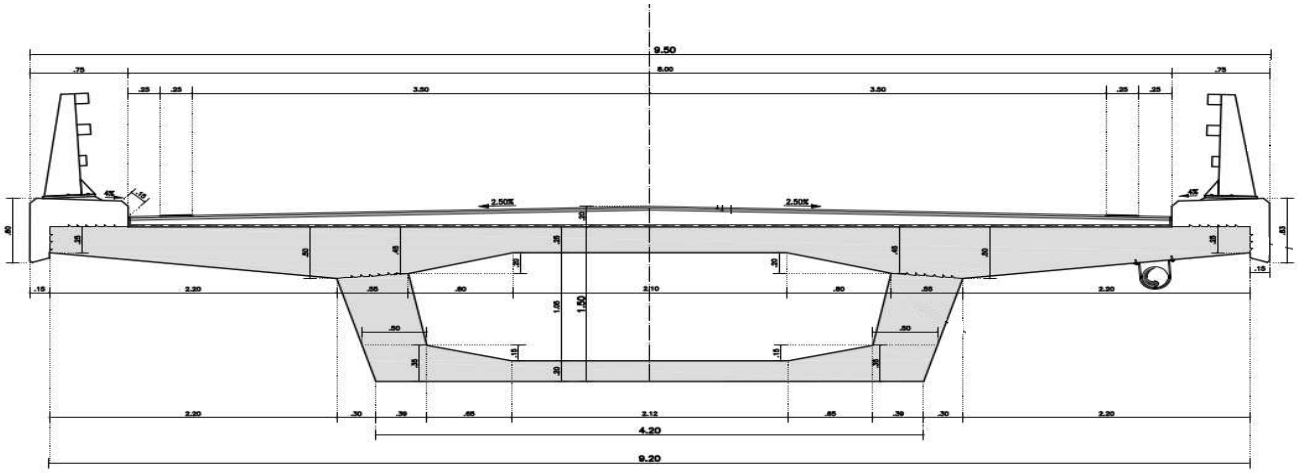


*Figure 10. Bridge considered: transverse section.*

A typical single-pier concrete bridge of mass $m_s = 723.9$ tn with two spans of 25 m each and conventional bearings is considered. The deck is 9.50 m wide. A schematic representation of the bridge is given in Figures 9 and 10. The damping factor of the system is equal to $c_s = 314.3443$ kNs/m, corresponding to reinforced concrete's damping ratio, $\zeta_s = 5\%$. Five conventional ALGABLOC NB 400x500/99/71 bearings are used, two above each one of the abutments and one above the pier, with a horizontal stiffness $k_b = 2730$ kN/m each. The total structure's stiffness is $k_o = 5x2730 = 13650$ kN/m. The natural period of the structure is calculated as follows

$$T_s = 2\pi\sqrt{\frac{m_s}{k_o}} = 1.45sec \tag{21}$$

At this point, it should be noted that in the approach presented hereby, the middle pier of the bridge is considered stiff enough to be neglected and the total structure's stiffness is considered to be equal to the horizontal stiffness of the bearings.

A possible implementation of the KDamper is presented in Figure 1. The equations of motion of the new system are Equations (2) and (3). As it has been described in the last paragraph of the previous section, parameter $\kappa$ is selected in order for the isolated system to have an eigenfrequency equal to 0.4 Hz. For the rest of the device's constants, the procedure presented previously is followed. Seven KDampers, working in parallel, are used to replace the conventional bearings. The full set of parameters, for each one of the seven KDampers, is presented in Table 1.

*Table 1. Full set of parameters for each one of the seven KDampers.*

| $\mu$ | $\kappa$ | $\rho$ | $\varepsilon$ | $\zeta_D$ | $k_R\ (kN/m)$ | $k_e\ (kN/m)$ | $k_N\ (kN/m)$ | $m_D\ (tn)$ | $c_D\ (kNs/m)$ |
|---|---|---|---|---|---|---|---|---|---|
| 0.05 | 3.2 | 1.0677 | 0.1558 | 0.616 | 3443.9 | 466.8 | -355.7 | 5.17 | 29.53 |

The system of Equations (2) and (3) is solved using the Newmark-β method with linear acceleration. A typical seismic ground acceleration is considered as shown in Figure 11. The dynamic response of the new linear system is presented in Figures 12 and 13, in terms of absolute accelerations and relative displacements, respectively, for both degrees of freedom (DoFs) (of the superstructure and of the internal one).

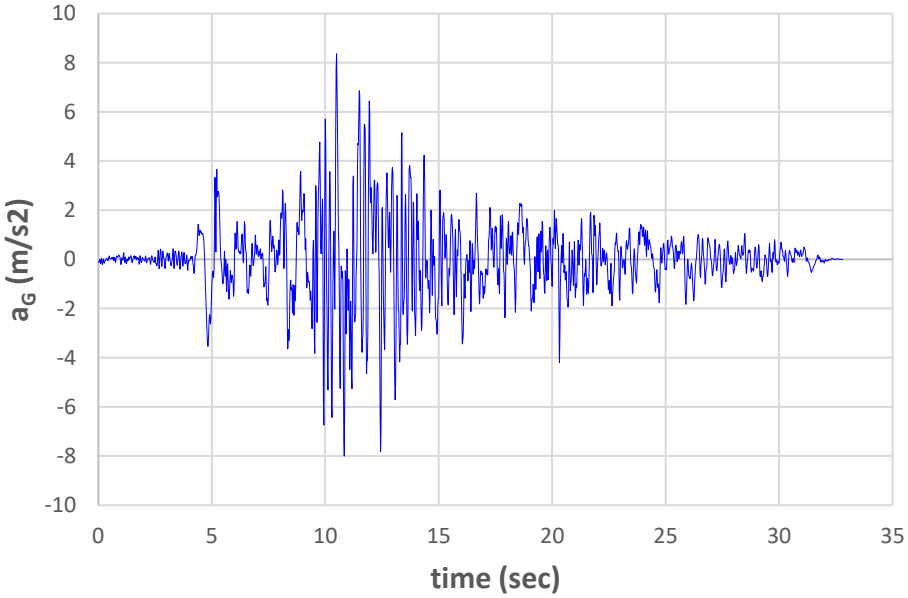


*Figure 11. Ground excitation acceleration considered (TABAS, $max|a_G| = 8.36\ m/s^2$).*

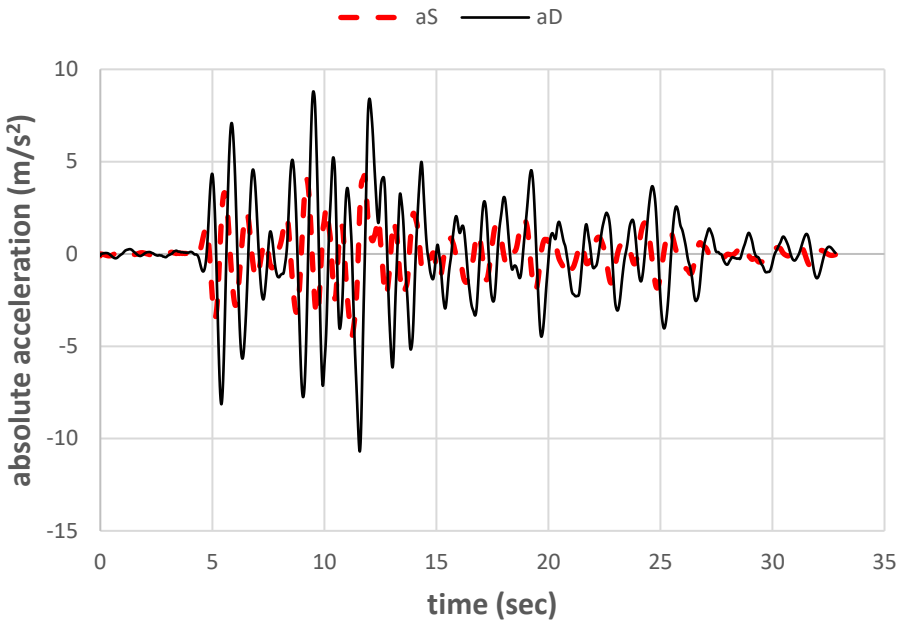


*Figure 12. Dynamic response of the isolated linear system, for both DoFs, in terms of absolute acceleration in m/s$^2$ ($max|a_S| = 4.46, max|a_D| = 10.70$).*

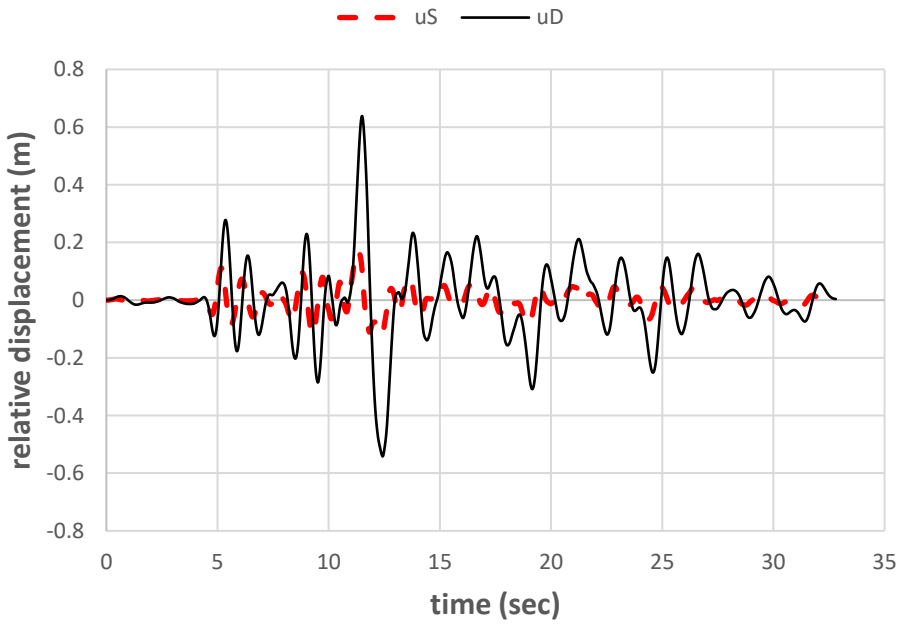


*Figure 13. Dynamic response of the isolated linear system, for both DoFs, in terms of relative displacement in m ($max|u_S| = 0.169, max|u_D| = 0.638$).*

The purpose of solving a linear dynamic problem first is to estimate the absolute maximum displacement of the internal degree of freedom (Dof) and approximate the value of the negative stiffness coefficient, in order to achieve the desired seismic mitigation effects. Depending on these two values, the negative stiffness element's set-up is selected. The mechanical design should render the system capable to reach the extreme value of displacement without becoming unstable. The ability to easily

implement such a design to the KDamper is also an important factor. In this specific test case, the absolute maximum value of the relevant displacement of the internal DoF is approximately 63.8 cm, as it can be derived from Figure 13.

**Indicative Implementation Of The KDamper**

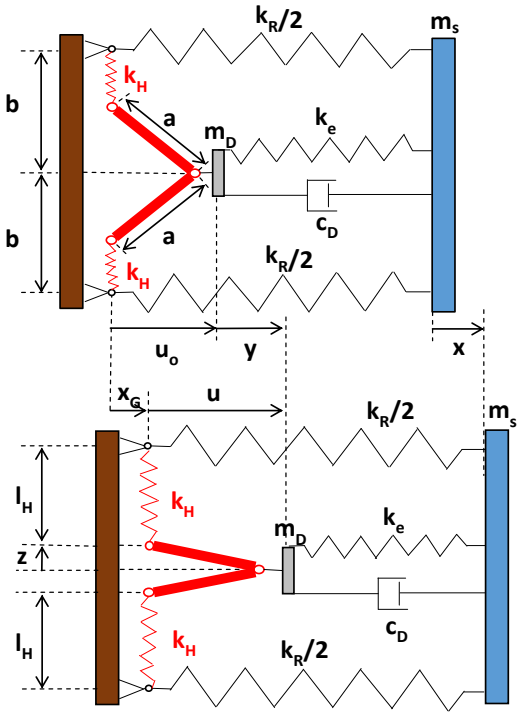


*Figure 14. Realization of the negative stiffness element by a set of pre-compressed springs (plan view).*

An example for an indicative implementation of the KDamper is depicted in Figure 14, where the static equilibrium position and the perturbed position after an external dynamic excitation $x_G(t)$ of the system are presented. The necessary notation concerning the various displacements of the system is also added to this schematic representation. The negative stiffness spring $k_N$ (shown in Figure 1) is realized by a set of two symmetric linear horizontal springs with coefficients $k_H$, which support the mass $m_D$ by an articulated mechanism. Precisely, the pair of springs with positive stiffness coefficient, $k_H$, generate a negative stiffness, $k_N$ given by

$$k_N = -2k_H\left[1 + c_I \frac{1}{\left(1-\frac{u_D^2}{a^2}\right)^{\frac{3}{2}}}\right] \tag{22}$$

where

$$c_I = \frac{(l_{HI}-b)}{a} \tag{23}$$

and the equations of motion of the proposed non-linear oscillator are

$$m_s\ddot{u}_s + (c_s + c_D)\dot{u}_s - c_D\dot{u}_D + (k_R + k_e)u_s - k_e u_D = -m_s a_G \tag{24}$$

$$m_D\ddot{u}_D - c_D\dot{u}_s + c_D\dot{u}_D - k_e u_s + k_e u_D + k_N u_D = -m_D a_G \tag{25}$$

In Equations (22) and (23), $a$ and $b$ are geometrical parameters of the mechanical design, whereas $l_{HI}$ is the initial length of the undeformed springs $k_H$. Further information on the detailed design of the elements of the mechanical configuration, depicted in Figure 14, can be found in Sapountzakis et al. (2016) and Sapountzakis et al. (2017). Following the same procedure for the hereby considered test case, the entire set of the parameters of the negative stiffness springs and mechanism is computed and presented in Table 2.

*Table 2. Negative stiffness spring and mechanism parameters for each one of the seven KDampers.*

| $k_H\ (kN/m)$ | $l_{HI}\ (m)$ | $a\ (m)$ | $b\ (m)$ | $u_o\ (m)$ |
|---|---|---|---|---|
| 177.9 | 1.540 | 0.7 | 1.575 | 0.005 |

**RESULTS**

The system of non-linear Equations (24) and (25) is also solved using the Newmark-β method with linear acceleration – a modified stiffness matrix is introduced at each step of the time iteration method. The same seismic ground acceleration as in the linear problem is considered, shown in Figure 11. The dynamic response of the proposed non-linear system is presented in Figures 15 and 16, for both DoFs (of the superstructure and internal), in terms of absolute accelerations and relative displacements, respectively. Moreover, comparative results between the initial SDoF and the isolated system are presented in Figures 17 and 18, again in terms of absolute accelerations and relative displacements respectively.

Considering the results presented in Figures 15 and 16, a consistency between the linear and non-linear solution of the isolated system is observed, confirming that the solution of the linear problem allows the user to obtain a preliminary design, before the specification of the special features and properties of the employed mechanism. Thus, the linear solution is valid regardless of the mechanical realization of the negative stiffness element that may differ from structure to structure. It is reminded here, that the negative stiffness behavior can be achieved by special mechanical designs involving conventional positive stiffness pre-stressed elastic mechanical elements, such as post-buckled beams, plates, shells and pre-compressed springs, arranged in appropriate geometrical configurations. The mechanical configuration used in the current effort is an indicative one.

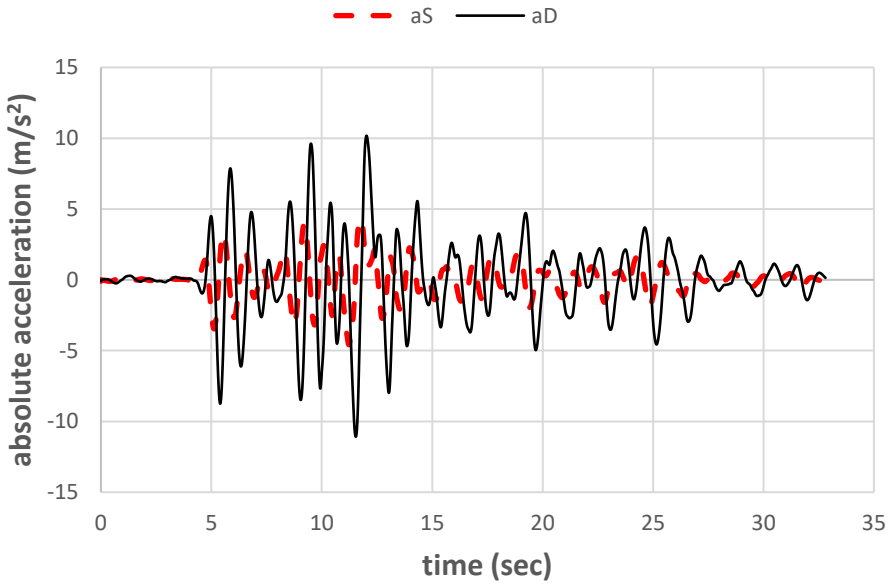


*Figure 15. Dynamic response of the isolated non-linear system, for both DoFs, in terms of absolute acceleration in m/s² ($max|a_S| = 4.58$, $max|a_D| = 11.08$).*

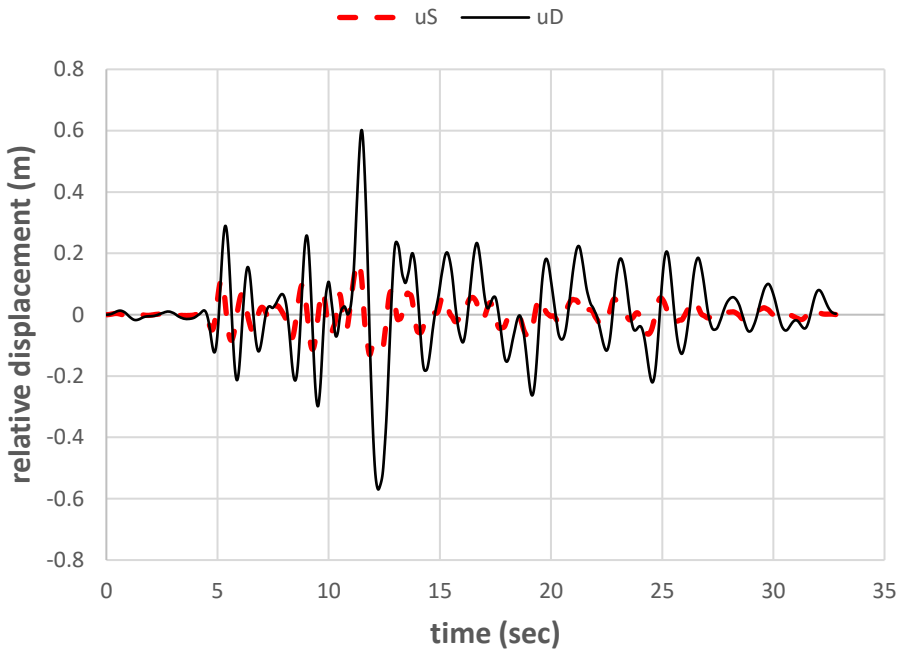


*Figure 16. Dynamic response of the isolated non-linear system, for both DoFs, in terms of relative displacement in m* ($max|u_S| = 0.17, max|u_D| = 0.60$).

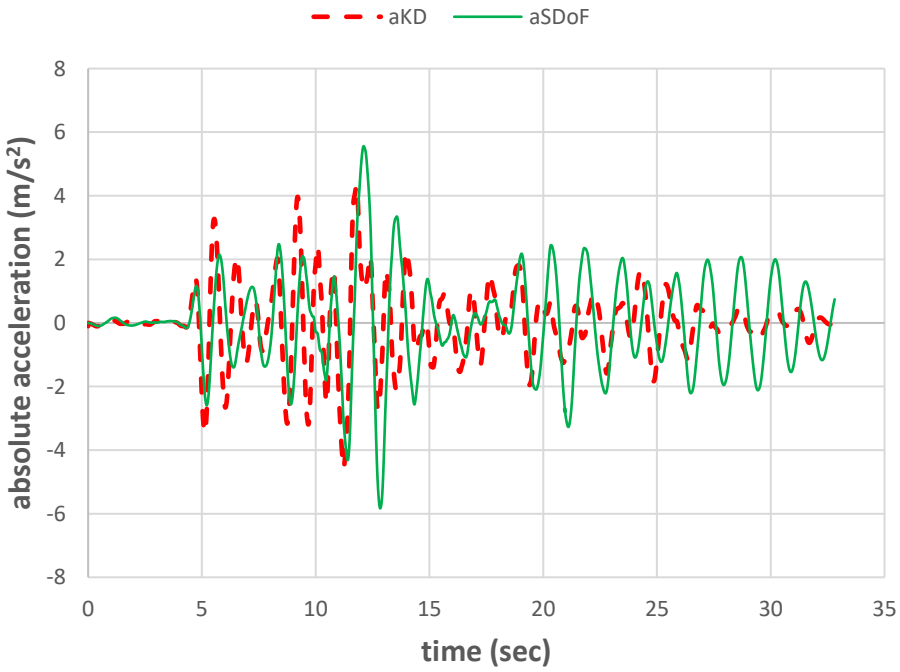


*Figure 17. Comparative results between the initial - SDoF and the isolated - KD system, in terms of absolute acceleration in m/s² (*$max|a_{SDoF}| = 5.83, max|a_{KD}| = 4.58$).

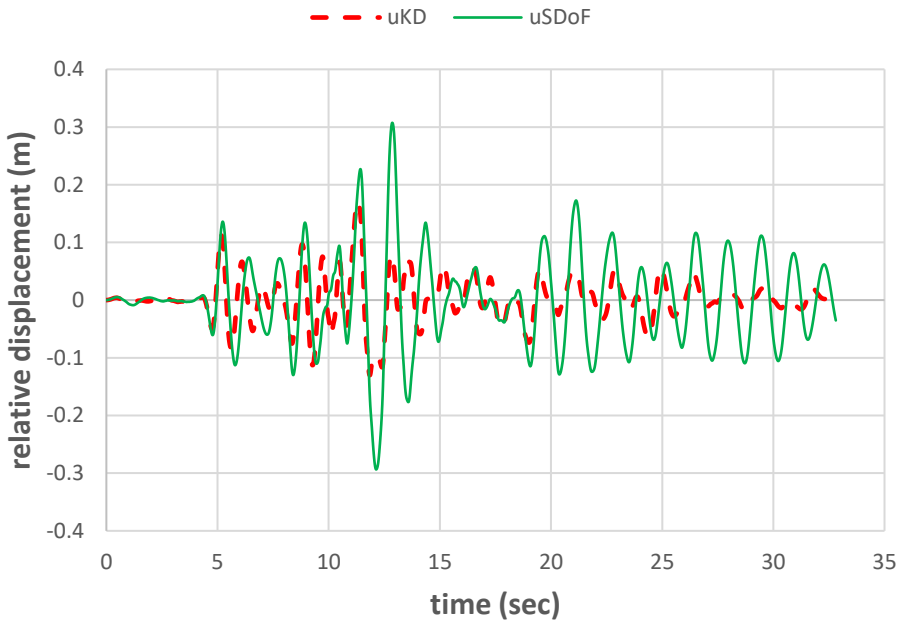


*Figure 18. Comparative results between the initial - SdoF and the isolated - KD system, in terms of relative displacement in m* ($max|u_{SDoF}| = 0.31, max|u_{KD}| = 0.17$).

Taking into account the comparative results between the initial SDoF and the isolated system after the implementation of the KDamper concept, as shown in Figures 17 and 18, the improved dynamic behavior of the structure is observed. More specifically an almost 50 % reduction of relative displacements is obtained, with a simultaneous decrease in terms of absolute acceleration. This drastic reduction is justified by the extraordinary damping properties that the KDamper concept exhibits. A calculation of the isolated system's new damping ratio can be found in the following section.

**Dynamic Features Of The Isolated System**

In this section, the dynamic features of the isolated – after the implementation of the KDamper concept – system are presented.

First of all, as it was mentioned in the previous, the new system exhibits extraordinary high properties. In order to calculate the isolated system's new damping ratio, the structure is subjected to a free vibration with initial conditions and the corresponding analysis is carried out. The dynamic response of the isolated system is depicted in Figure 19. The value of the new damping ratio is calculated as in Equation (26).

$$ln\left[\frac{u_s(t)}{u_s(t+T)}\right] = \frac{2\pi\zeta}{\sqrt{1-\zeta^2}} \tag{26}$$

where $T$ is the time between two consecutive peaks of the dynamic response of the system, as shown in Figure 19. The new damping ratio results equal to 26.8%, as mentioned in Table 3. It should be noticed here, that a 5 times larger damping ratio is obtained. The damping ratio is also kept lower than 30%, in order to avoid coupling phenomena due to higher order modes interference (Kelly (1999)).

In Table 3, the dynamic eigenfeatures and especially, the eigenfrequency and eigenperiod of both the initial SDoF and the isolated structures are presented, enabling comparisons to be made. Finally, the transfer functions of both systems are given in Figures 20 and 21, in terms of acceleration and displacement, respectively, validating that the proposed design demonstrates an overall enhanced dynamic performance.

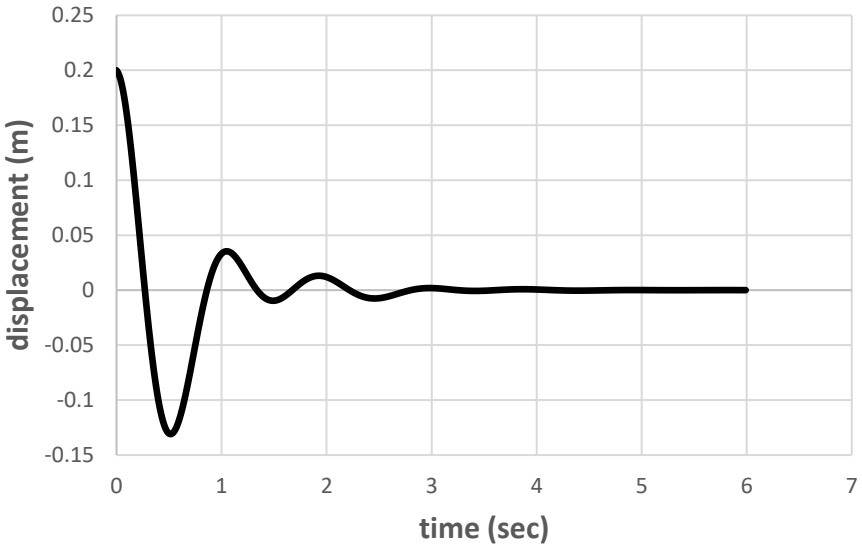


*Figure 19. Dynamic response of the isolated system to a free vibration with initial conditions.*

*Table 3. Dynamic features of the initial – SDoF and the isolated systems/structures.*

| | Eigenperiod $T$ $(sec)$ | Eigenfrequency $f$ $(Hz)$ | Damping ratio $\zeta$ (%) |
|---|---|---|---|
| Initial – SDoF system | 1.45 | 0.70 | 5 |
| Isolated system | 2.32 | 0.43 | 26.8 |

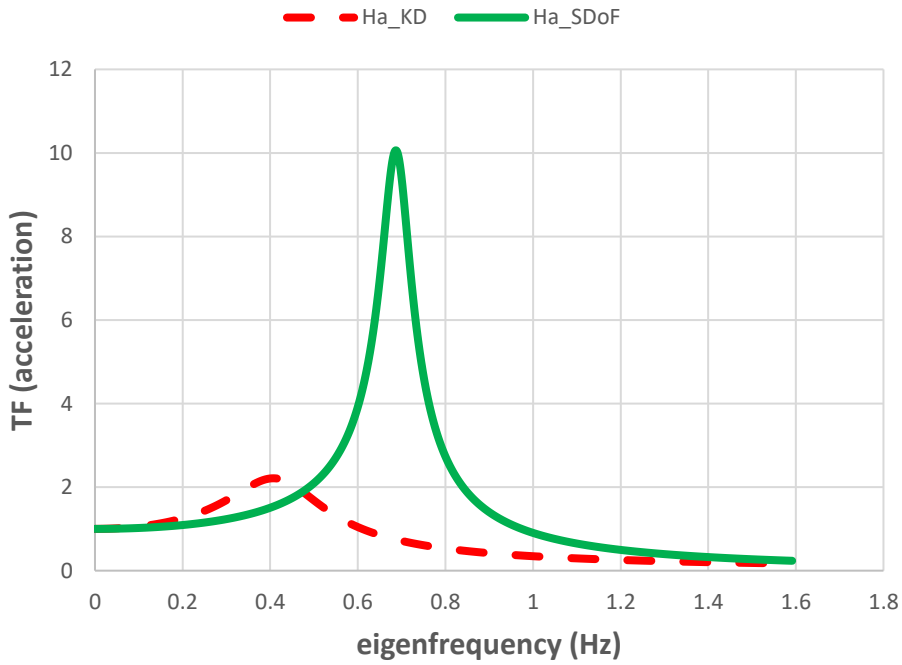


*Figure 20. Transfer functions of the initial – SdoF and the isolated – KD systems, in terms of acceleration.*

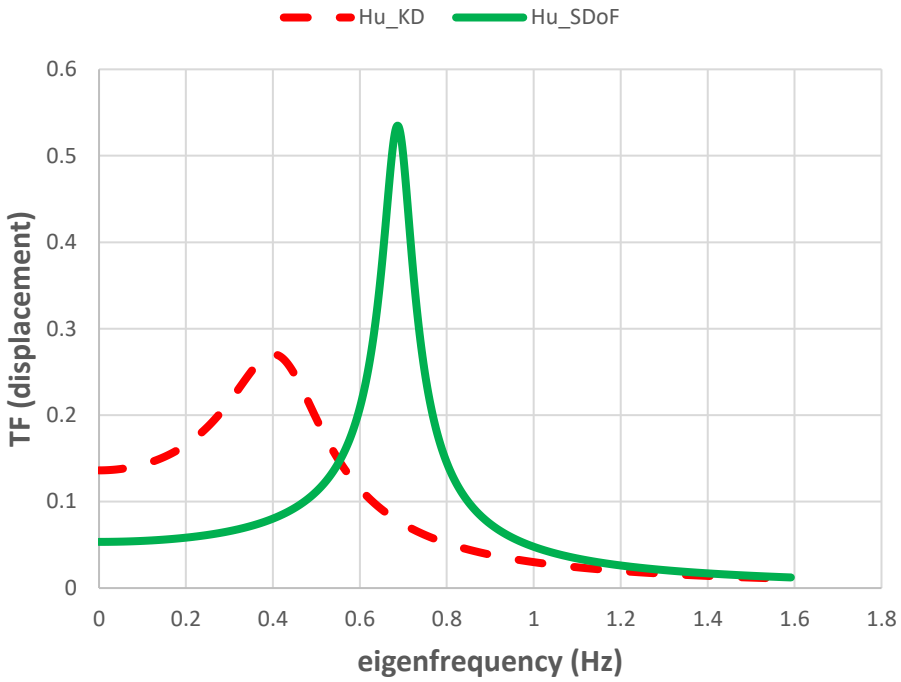


*Figure 21. Transfer functions of the initial – SdoF and the isolated – KD systems, in terms of displacement.*

## CONCLUSION

In this paper, the implementation of a novel passive vibration absorption and damping concept, entitled KDamper concept, to a typical concrete bridge structure was presented. The design of the proposed device has been based on the frequential characteristics of the system. Time history analysis under seismic excitation was carried out. The dynamic response of the new isolated system, as well as, its dynamic eigenfeatures have been presented and compared with the corresponding ones belonging to the initial SDoF system.

Taking into account all the data presented in the results section, the following concluding remarks can be made:

- The isolated system exhibits extraordinary damping properties, due to the five times higher damping ratio as compared to the initial one.
- A drastic reduction of deck's displacements (almost 50%) has been achieved.
- The proposed design has been based on the desired frequential characteristics of the isolated system. This way an overall improved dynamic behavior, both in terms of absolute acceleration and relative displacement has been accomplished.
- The comparison between the linear and non-linear solution confirms that the linear model is accurate enough to be used for preliminary design purposes, regardless of the specific features of the mechanical realization of the negative stiffness element.

Summarizing the previous, the KDamper concept seems to be the most promising alternative to conventional seismic isolation techniques, offering a user-friendly and adjustable to any structure design procedure at the same time. Finally, the KDamper concept is easy to implement, whereas its effectiveness and robustness render it a helpful tool for engineers.

## REFERENCES


Antoniadis, I., Chronopoulos, D., Spitas, V. and Koulocheris, D. (2015). "Hyper-damping properties of a stable linear oscillator with a negative stiffness element." *J. Sound and Vib*, 346, 37-52

Antoniadis, I., Kanarachos, S., Gryllias, K. and Sapountzakis, I., (2016). "KDamping: a stiffness based vibration absorption concept." *J. Vib. And Control*.

Carella, A., Brennan, M. and Waters, T. (2007). "Static analysis of a passive vibration isolator with quasi-zero-stiffness characteristic." *J. Sound and Vib*, 301, 678-689.

Debnath, N., Deb, S.K. and Dutta, A (2015). "Multi-modal vibration control of truss bridges with tuned mass dampers under general loading." *J. of Vib. and Control*.

Den Hartog, J. P. (1956). *Mechanical Vibrations,* 4th Ed., McGraw-Hill, New York.

Frahm, H. (1909). *Device for damping vibrations of bodies*, US patent #989958

Haskett, T., Breukelman, B., Robinson, J. and Kottelenberg, J. (2003). *Tuned mass dampers under excessive structural excitation*, Report of the Motion. Inc. Guelph, Ontario, Ca.

Ibrahim, R. (2008). "Recent advances in nonlinear passive vibration isolators." *J. of Sound and Vib*, 314, 371-452.

Kelly, J. M., (1999). "The role of damping in seismic isolation." *Earth. Eng. and Struct. Dyn.*, 28, 3-20.

Luft, R. W., (1977). "Tuned mass dampers for buildings." *J. Struct. Div.*, 105, 2766-2772.

McNamara, R. J., (1979). "Optimal tuned mass dampers for buildings." *J. Struct. Div.*, 103, 1985-1998.

Platus, D. L. (1999). "Negative-stiffness-mechanism vibration isolation systems." *Proc. SPIE's Int. Symp. on Optical Science, Eng. and Instrumentation*, 98-105.

Qin, L., Yan, W., and Li, Y. (2009). "Design of frictional pendulum TMD and its wind control effectiveness." *J. Earth. Eng. And Eng. Vib.*, 20, 153-157.

Sapountzakis, E. I., Syrimi, P. G., Pantazis, I. A. and Antoniadis, I. A. (2016). "KDamper concept in seismic isolation of bridges." *Proc. of the 1st Int. Conf. on Nat. Hazard and Infrastruct.*, ICONHIC, Chania, Crete, Greece.

Sapountzakis, E. I., Syrimi, P. G., Pantazis, I. A. and Antoniadis, I. A. (2017). "KDamper concept in seismic isolation of bridges with flexible piers." *Eng. Str.*, 153, 525-539.

Weber, B., and Feltrin, G. (2010). "Assessment of long-term behaviour of tuned mass dampers by system identification." *Eng. Str.*, 32, 3670-3682.

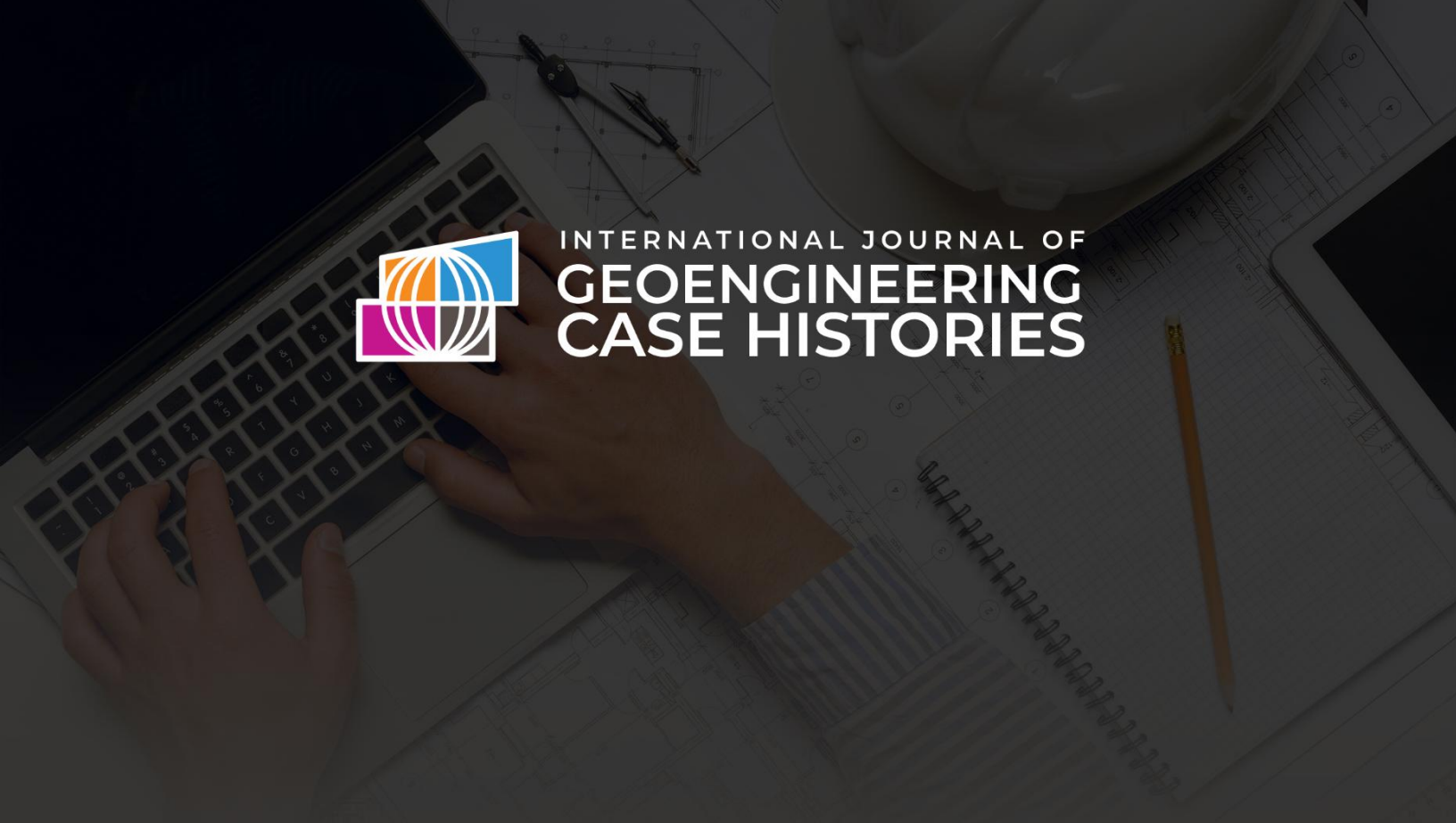

INTERNATIONAL JOURNAL OF
GEOENGINEERING
CASE HISTORIES

***The Journal's Open Access Mission is generously supported by the following Organizations:***

dar

Geosyntec consultants
engineers | scientists | innovators

CONETEC
MUD CAT DRILLING
LANKELMA
Geotech DRILLING

ENGEO
Expect Excellence